Characterization of Dielectric Materials at WR-15 Band (50–75 GHz) Using VNA-Based Technique

Yi Wang, *Student Member, IEEE*, Xiaobang Shang, *Senior Member, IEEE*, Nick M. Ridler, *Fellow, IEEE*, Tongde Huang, and Wen Wu, *Senior Member, IEEE*

***Abstract*— This article presents an in-depth study of a new vector network analyzer (VNA)-based electromagnetic material measurement method relying on a commercially available material characterization kit (MCK). These MCKs provide effectively a guided free-space technique with less stringent requirement on alignment compared with conventional free-space techniques. Coupled with time gating, these MCKs employ a simple calibration, composed of reflect and thru standards only, prior to taking reflection and transmission S-parameter measurements. This MCK-based method complements other conventional measurement techniques, e.g., time-domain spectroscopy (TDS) and resonant cavity, allowing fast broadband dielectric material characterization over the millimeter- and submillimeter-wave frequency ranges. In this article, a WR-15 (50–75 GHz) MCK is utilized for the measurements of S-parameters for seven types of low-loss dielectric material. Their dielectric constant and loss tangent are extracted from S-parameters and are compared against literature values. A relatively good agreement is achieved. Moreover, an investigation into the uncertainties of the extracted dielectric constant and loss tangent is performed and reported.**

***Index Terms*— Dielectric constant, dielectric measurements, free-space measurement, loss tangent, millimeter-wave measurements, vector network analyzer (VNA).**

I. Introduction

CHARACTERIZATIONS of low-loss dielectric material properties, such as dielectric constant ε' and loss tangent $\tan\delta$, are of great importance for a variety of applications, including resonators, filters, lenses, substrates, and imaging [1], [2]. There exist many different measurement methods for different types of dielectric materials and different frequency bands, and all these methods have their own advantages and disadvantages [3]. These methods may be classified into a few common types, including parallel-plate capacitor [4], coaxial probe [5], [6], resonant cavity [7], [8], transmission line [9], [10], and free space [2], [11], [12]. The parallel-plate capacitor method measures the change in capacitance between the parallel plates, where the material is inserted between the plates, and calculates the dielectric constant and loss tangent from the change due to the insertion of the material. This method is usually used at the relatively lower frequencies, i.e., below 1 GHz [4], [12]. For the conventional coaxial probe method, fringing electromagnetic fields are launched from the open end of the probe into the dielectric specimen, and the dielectric constant and loss tangent are estimated from the reflection coefficient of the TEM-wave at the end of the probe [3]. Coaxial probes are widely used for noninvasive dielectric measurement of liquids, soft semisolids, and even flat hard solids. However, this technique is generally only effective for measurements below 50 GHz [13]. The resonant cavity method, an inherently narrowband method, determines the dielectric constant and loss tangent from the measurement of resonant frequency and quality factor (Q-factor) of a cavity resonator, both empty and with the specimen inserted into the resonator. This method provides the best loss tangent resolution over a narrow range of frequencies [3]. The transmission-line method uses the lines (usually coaxial and waveguide) as sample holders and calculates the dielectric constant and loss tangent from the reflection and transmission of the line. This is a broadband method and is suitable for measurements up to millimeter-wave frequencies. However, the sample preparation tends to be difficult when the frequency rises to millimeter wave and above (i.e., when the size of the transmission line is very small).

The free-space measurement method is widely utilized for low-loss dielectric characterization at millimeter-wave frequencies and beyond, and this method is nondestructive, noncontacting, and broadband [1], [2], [11], [14]. This technique operates in a similar way to the above-mentioned transmission-line technique and uses the same methods to calculate dielectric constant and loss tangent. The free-space technique calculates the dielectric constant and loss tangent from the reflection and transmission S-parameters measured

Manuscript received June 22, 2019; revised September 16, 2019; accepted November 5, 2019. Date of publication November 20, 2019; date of current version June 9, 2020. This work was supported by the European Metrology Programme for Innovation and Research (EMPIR) Project 18SIB09 Traceability for electrical measurements at millimetre-wave and terahertz frequencies for communications and electronics technologies. The EMPIR Programme is co-financed by the Participating States and from the European Union's Horizon 2020 Research and Innovation Programme. The Associate Editor coordinating the review process was Leonid Belostotski. *(Corresponding authors: Xiaobang Shang; Nick M. Ridler.)*

Y. Wang is with the School of Electronic and Optical Engineering, Nanjing University of Science and Technology, Nanjing 210094, China (e-mail: wangyi@njust.edu.cn).

X. Shang and N. M. Ridler are with the National Physical Laboratory, Teddington TW11 0LW, U.K. (e-mail: xiaobang.shang@npl.co.uk; nick.ridler@npl.co.uk).

T. Huang and W. Wu are with the Nanjing University of Science and Technology, Nanjing 210094, China (e-mail: tongdeh@njust.edu.cn; wuwen@njust.edu.cn).

Color versions of one or more of the figures in this article are available online at http://ieeexplore.ieee.org.

Digital Object Identifier 10.1109/TIM.2019.2954010

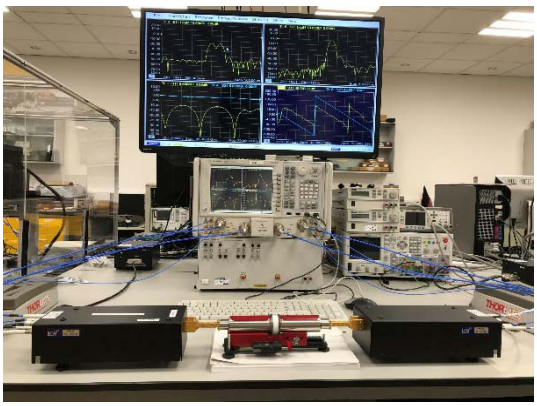

(a)

(b)

Fig. 1. Photographs of the WR-15 (50–75 GHz) MCK-based experimental apparatus. (a) Overview of the whole measurement system, comprising VNA, WR-15 extension heads, and the WR-15 MCK. (b) Close-up view of the WR-15 MCK, showing a sample of PTFE sandwiched between the two MCK test ports.

for a material that is placed between the transmit and receive antennas. Typically, either parabolic mirrors [2] or lenses [1] are employed (between these antennas) to prevent divergence of the beam. Time-domain spectroscopy (TDS) [15], [16] is another popular technique based on free-space measurement. TDS has several appealing advantages, including relatively low cost and the applicability of the measurement technique over a wide frequency range [17]. However, generally, the TDS method is less accurate than vector network analyzer (VNA)-based techniques that provide lower signal-to-noise ratios [3]. Such free-space techniques suffer from two main disadvantages. First, high-precision micrometer positioners are needed to carry out the relevant free-space calibrations that are typically nontrivial [2]. Second, the measurement system usually takes up a large amount of laboratory space [3].

Recently, new commercial material characterization kits (MCKs), developed by SWISSto12, have become available for waveguide frequency bands from 50 GHz to 1.1 THz. This broadband method is effectively a guided free-space approach. During measurement, the material is sandwiched between the two antennas that comprise the test ports of the MCK, as shown in Fig. 1. This minimizes the efforts needed for sample preparation. In contrast to most conventional free-space measurement setups, these MCKs eliminate the need for large parabolic mirrors or lens, and therefore, this significantly reduces the overall size of the measurement system. Note that these MCKs are not ideally suited to measure samples at varying temperatures—in these scenarios, the conventional free-space technique is likely to be more effective. An initial assessment of an MCK was described in [18]. However, only preliminary results were reported in [18], without any in-depth discussions or analyses. This article reports on a comprehensive investigation into material characterization using an MCK at WR-15 band (50–75 GHz). Common low-loss dielectric materials—PTFE, TPX, HDPE, Alumina, Silicon, Astra MT77 [19], and Rogers 3003 [20]—are measured with the MCK and the results are presented and compared with other sources of information. In addition, for PTFE, samples with different thicknesses are prepared, measured, and discussed, to explore the impact of sample thickness on achieved measurement quality. Finally, the uncertainties in the extracted dielectric constant and loss tangent values are calculated and reported. To the best of our knowledge, this is the first time that an in-depth study of material characterization using MCKs has been reported.

This article is organized as follows. In Section II, the measurement technique is introduced. Section III describes the measurement results for the abovementioned dielectric samples. Section IV presents an uncertainty analysis for the extracted dielectric constant and loss tangent, which is followed by conclusions in Section V.

II. Guided Free-Space Measurement Technique

Fig. 1(a) shows the MCK measurement setup at NPL. A pair of Virginia Diodes Inc. (VDI) WR-15 frequency extenders are connected to a Keysight Technologies N5247A PNA-X network analyzer, enabling measurements of *S*-parameters in the WR-15 waveguide band. The N5247A PNA-X Network Analyzer enables S-parameter measurements from 10 MHz to 67 GHz, whereas the VDI frequency extenders allow measurement at other frequency ranges, including 50–75 GHz. The MCK has standard UG-387/UM waveguide flanges and can be connected to the frequency extenders directly. The MCK itself, as shown in Fig. 1(b), is a fixture formed of two identical corrugated horn antennas, with the inner and outer radius of 4.1 and 4.526 mm, respectively. These corrugated horn antennas operate in the HE_{11} mode (with ultralow propagation loss) and are capable of launching a 98% pure Gaussian beam [21], [22]. The MCK also includes the transitions that convert the TE_{10} mode at the input to the standard rectangular waveguide to the HE_{11} mode at the input to the corrugated horn antennas.

During measurement, a dielectric material is placed in the gap between the two antennas, which can be gradually opened and closed using a gap adjustment mechanism. Similar to the conventional free-space measurement system, the MCK produces a Gaussian beam that provides plane-wave illumination of the sample [21]. However, compared to a conventional free-space measurement system, the MCK allows the electromagnetic wave to propagate within an enclosed low-loss environment and removes the need for bulky mirrors or lenses.

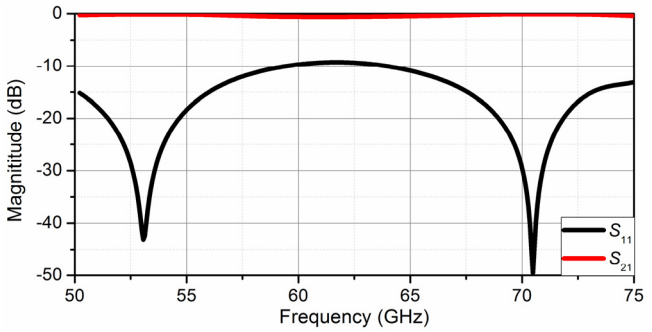

Fig. 2. Measured S-parameters for PTFE sample (of thickness 5.99 mm).

The gated-reflect-line (GRL) calibration technique [23] is carried out at the ends of the antennas prior to making measurements of S-parameters. The GRL method requires a simple zero-length "Thru" standard and a metallic reflecting plate as the "Reflect" standard [23]. The "Thru" standard is realized by closing the gap between the two halves of the corrugated antennas. The "Reflect" standard is realized by placing a short circuit (a 1-mm-thick metal shim, provided with the MCK) between the two halves of the antennas. Time-domain gating, a useful technique for free-space measurements, is employed here to separate the wanted signals from the spurious reflections generated elsewhere in the measurement system (e.g., due to the connections between the MCK and the test ports of the VNA, and so on). In this article, the time-gating window is set to 400 ps, i.e., the value recommended by the manufacturer of the MCK [21].

S-parameter measurements were taken after the abovementioned calibration. The VNA was set to measure at 501 frequency points with an intermediate-frequency (IF) bandwidth of 50 Hz. No VNA averaging was used for the measurements. All measurements were carried out at a laboratory temperature of 23 °C ± 1 °C. As with conventional free-space methods or other traveling-wave methods, the dielectric constant (ε') generally depends upon the measured phase change and the loss tangent (tanδ) generally depends upon the measured attenuation of the beam when the material sample is present [3]. Details about how to extract the dielectric constant and loss tangent from measured S-parameters are described in Section III.

III. Comparisons

Seven different kinds of common dielectric material were measured using the MCK over the frequency range 50–75 GHz. These materials are PTFE, TPX, HDPE, Alumina, Silicon, Astra MT77, and Rogers 3003. The latter two are popular low-loss dielectric materials for substrates of millimeter-wave printed circuits.

A. Algorithms to Extract Permittivity From S-Parameters

Software is supplied with the MCK for data analysis, which allows computation of the dielectric constant and loss tangent directly from measured S_{11} and S_{21} (or S_{22} and S_{12}). Fig. 2 shows the measured S_{11} and S_{21} of PTFE (of thickness 5.99 mm). In addition, a well-known algorithm

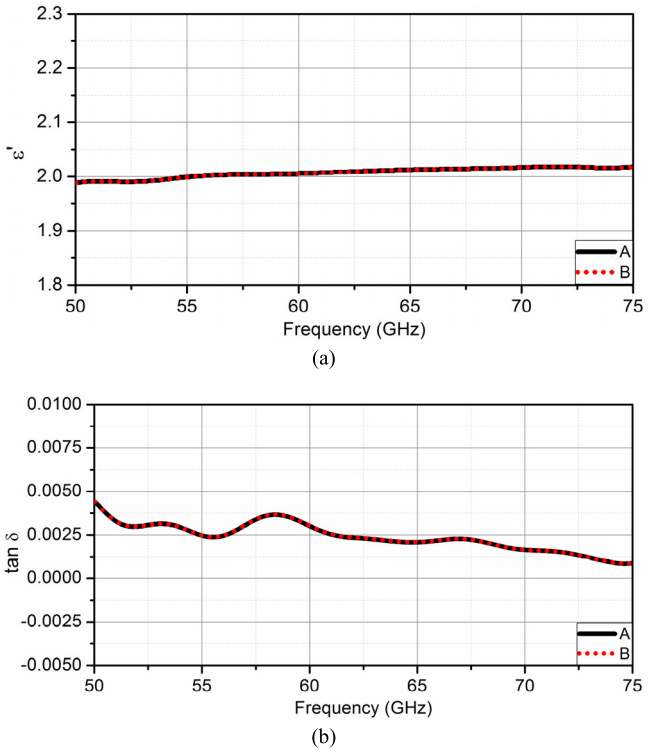

Fig. 3. Extracted (a) dielectric constant ε' and (b) loss tangent tanδ for PTFE sample using two different algorithms. Line A corresponds to MCK software; Line B represents the NIST precision model (using transmission data only).

(NIST precision model [24]) has been used to calculate the dielectric constant and loss tangent from the measured S-parameters for the PTFE sample (of thickness 5.99 mm). This is to verify the reliability of the results extracted using the software supplied with the MCK. Fig. 3 shows a comparison of the dielectric constant and loss tangent values extracted using these two algorithms. It can be seen that the results extracted using the MCK software agree extremely well with those extracted using the NIST precision model.

A further comparison between the MCK software and the NIST precision model was undertaken using two other samples: silicon (of thickness 3.06 mm) and alumina (of thickness 10.18 mm). The results are shown in Figs. 4 and 5, respectively. Again, excellent agreement between these two approaches is achieved. A magnified view of a part of the extracted dielectric constant for silicon (shown in the inset in Fig. 4) shows steps in the results obtained using the MCK software. This is due to the limited numerical precision specified in the MCK software. The comparison of algorithms demonstrates that the results extracted from MCK software are consistent with those obtained using the NIST precision model based on transmission only.

The key equations in the NIST precision model [24] are briefly described next. The absolute permittivity ε and permeability μ of a dielectric material can be expressed as

$$\varepsilon = [\varepsilon' - j\varepsilon'']\varepsilon_0 = \varepsilon^*\varepsilon_0 \tag{1}$$

$$\mu = [\mu' - j\mu'']\mu_0 = \mu^*\mu_0 \tag{2}$$

where ε_0 and μ_0 are the permittivity and permeability of vacuum, respectively, ε^* and μ^* are the complex permittivity

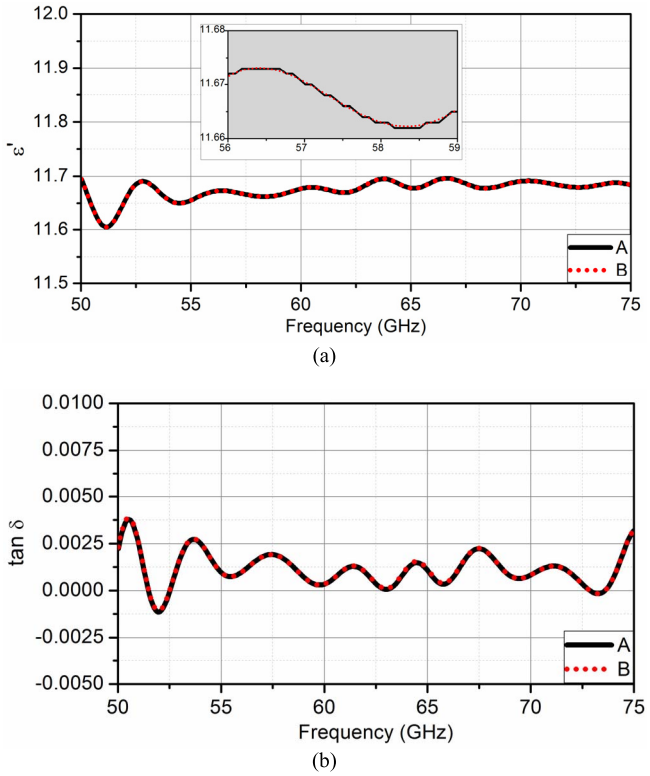

Fig. 4. Extracted (a) dielectric constant ε' and (b) loss tangent tanδ for silicon sample using two different algorithms. Line A corresponds to the MCK software; Line B corresponds to the NIST precision model (using transmission data only).

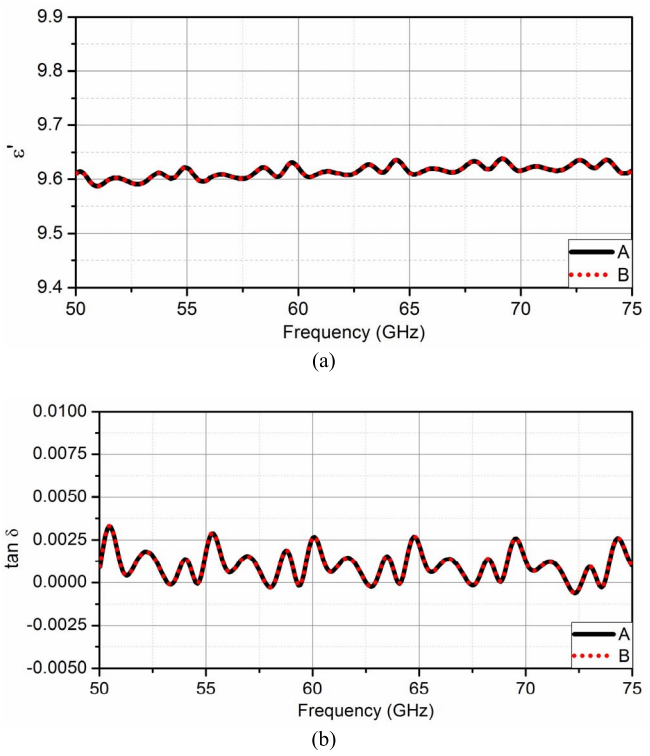

Fig. 5. Extracted (a) dielectric constant ε' and (b) loss tangent tanδ for the alumina sample using two different algorithms. Line A corresponds to the MCK software; Line B corresponds to the NIST precision model (using transmission data only).

and permeability relative to a vacuum, respectively, ε' and ε'' are the real and imaginary components of the complex relative permittivity, respectively, and μ' and μ'' are the real and imaginary components of the complex relative permeability, respectively. The loss tangent tanδ is calculated as $\varepsilon''/\varepsilon'$. The propagation constant is utilized to link the permittivity to the S-parameters. The propagation constants in vacuum (γ_0) and in material (γ) are given as

$$\gamma = j\sqrt{\frac{\omega^2\mu^*\varepsilon^*}{c^2} - \left(\frac{2\pi}{\lambda_c}\right)^2} \tag{3}$$

$$\gamma_0 = j\sqrt{\left(\frac{\omega}{v}\right)^2 - \left(\frac{2\pi}{\lambda_c}\right)^2} \tag{4}$$

where c and v are the speed of light in vacuum and in material, respectively, ω is the angular frequency, and λ_c is the cutoff wavelength. The reflection coefficient Γ and the transmission coefficient T can be expressed as

$$\Gamma = \frac{\frac{\gamma_0}{\mu_0} - \frac{\gamma}{\mu}}{\frac{\gamma_0}{\mu_0} + \frac{\gamma}{\mu}} \tag{5}$$

$$T = \exp(-\gamma L) \tag{6}$$

where L is the sample thickness. The dielectric constant and loss tangent can be determined by solving the following equation, in an iterative fashion [24], using a reference value in the literature as the initial estimate:

$$\frac{1}{2}\{[S_{12} + S_{21}] + \beta[S_{11} + S_{22}]\} = \frac{T(1-\Gamma^2) + \beta\Gamma(1-T^2)}{1 - T^2\Gamma^2}. \tag{7}$$

β is a constant, which varies as a function of the sample thickness, the uncertainty in the S-parameters, and the loss characteristics of the material [24]. In this article, β is set to zero, which means that only transmission data (S_{21} or S_{12}) obtained by measurements is used during the calculation of the dielectric constant and loss tangent. This is a sensible assumption, in which for low-loss materials, the magnitude of S_{11} (or S_{22}) is very small and so the S_{21} (or S_{12}) signal dominates [24].

B. Sample Results

Fig. 6 shows the extracted dielectric constant and loss tangent for Astra MT77 sample (thickness 1.60 mm) and Rogers 3003 sample (thickness 1.50 mm) over the frequency range of 50–75 GHz. Similarly, Fig. 7 shows the extracted dielectric constant and loss tangent for the HDPE sample (thickness 5.97 mm) and TPX sample (thickness 2.81 mm). Tables I and II summarize the results extracted using the MCK. Tables I and II also show the selected values reported in the literature. The values of dielectric constant, presented in Table I, show good agreement between the MCK measured values and the values found in the literature. The values of loss tangent, presented in Table II, also show acceptable agreement,

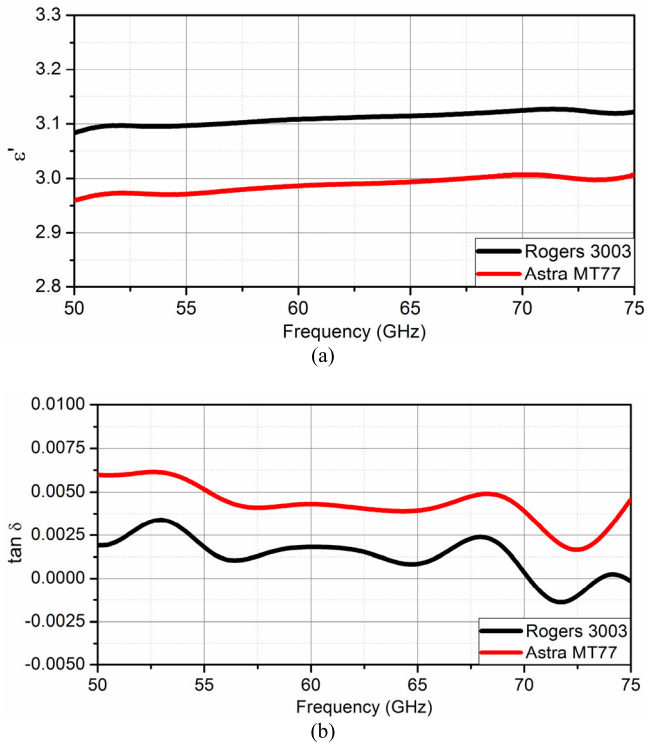

Fig. 6. Extracted (a) dielectric constant ε' and (b) loss tangent tanδ, for Astra MT77 sample (thickness 1.60 mm) and Rogers 3003 (thickness 1.50 mm), using NIST precision model (transmission only).

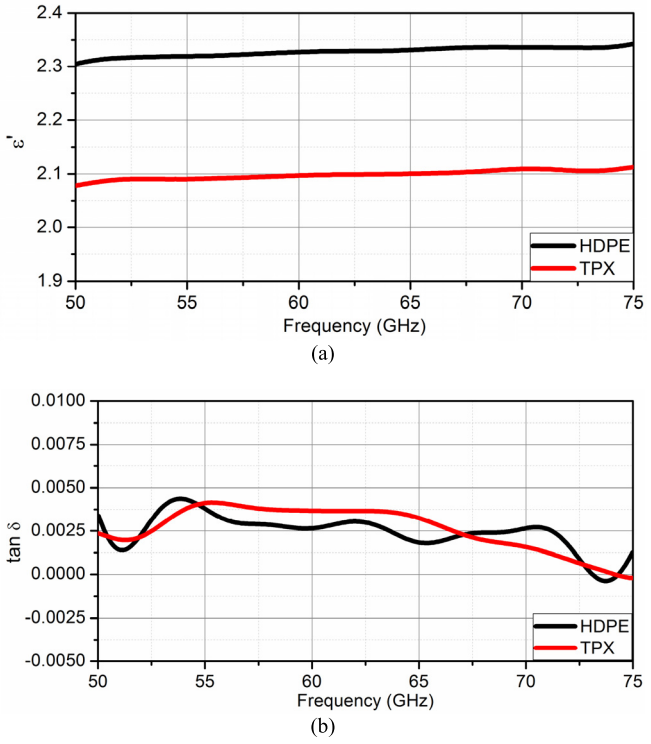

Fig. 7. Extracted (a) dielectric constant ε' and (b) loss tangent tanδ, for HDPE sample (thickness 5.97 mm) and TPX (thickness 2.81 mm), using the NIST precision model (transmission only).

although some of these values from the literature are very close to zero. Apart from the different thicknesses of the samples, sample measurement angle, and test frequency, the differences between our results and values found in the literature may be attributed to factors, such as measurement setup, extraction process, surface roughness of the samples, and differences in sample manufacturing/preparation. The uncertainties in the extracted dielectric constant and loss tangent values may account for these differences. This will be discussed in Section IV.

TABLE I

EXTRACTED DIELECTRIC CONSTANT VALUES, AVERAGED OVER FREQUENCY, COMPARED WITH VALUES FOUND IN THE LITERATURE

Sample	Thickness (mm)	ε' (extracted)	ε' (literature)
PTFE	5.99	2.008	2.1 @ 12 GHz, [25] 2.06 @ 92.5 GHz, [26]
Astra MT77	1.60	2.988	3.0 @ 79 GHz, [19] 3.0 @ 10 GHz, [27]
Rogers 3003	1.50	3.110	3.0 @ 60 GHz, [20] 3 @ 10 GHz, [28]
TPX	2.81	2.099	2.13 @ 38 GHz, [29] 2.136 @ 700 GHz, [30]
HDPE	5.97	2.301	2.3 @ 700 GHz, [30] 2.2505 @ 85 GHz, [31]
Alumina	10.18	9.618	9.4 @ 2.5 THz, [33] 9.424 @ 17 GHz, [32]
Silicon	3.06	11.678	11.7 @ 700 GHz, [30] 11.67 @ 1 THz, [33]

TABLE II

EXTRACTED LOSS TANGENT VALUES, AVERAGED OVER FREQUENCY, COMPARED WITH VALUES FOUND IN THE LITERATURE

Sample	Thickness (mm)	tan δ (extracted)	tan δ (literature)
PTFE	5.99	0.002	0.000 3 @ 12 GHz, [25] 0.000 389 @ 92.5 GHz, [26]
Astra MT77	1.60	0.004	0.001 7 @ 79 GHz, [19] 0.001 7 @ 10 GHz, [27]
Rogers 3003	1.50	0.001	0.001 3 @ 60 GHz, [20] 0.001 3 @ 10 GHz, [28]
TPX	2.81	0.003	0.004 3 @ 38 GHz, [29] 0.001 74 @ 700 GHz, [30]
HDPE	5.97	0.002	0.000 224 @ 700 GHz, [30] 0.000 225 217 @85 GHz, [31]
Alumina	10.18	0.001	0.021 @ 2.5 THz, [33] 0.000 31 @ 17 GHz, [32]
Silicon	3.06	0.001	0.000 26 @ 700 GHz, [30] 0.000 4 @ 1 THz, [33]

IV. UNCERTAINTIES

The extracted dielectric constant and loss tangent values, reported in Tables I and II, are subject to several sources of error. These errors will cause the extracted values to differ from the underlying true values of these quantities. In order to quantify the extent of the difference between the extracted values and the true values, it is useful to provide an estimate of the likely uncertainty in the extracted values.

This section provides the preliminary estimates of the uncertainty due to the main sources of error, which include the insertion repeatability of the sample into the sample holder, the sample thickness, the measurement of the sample

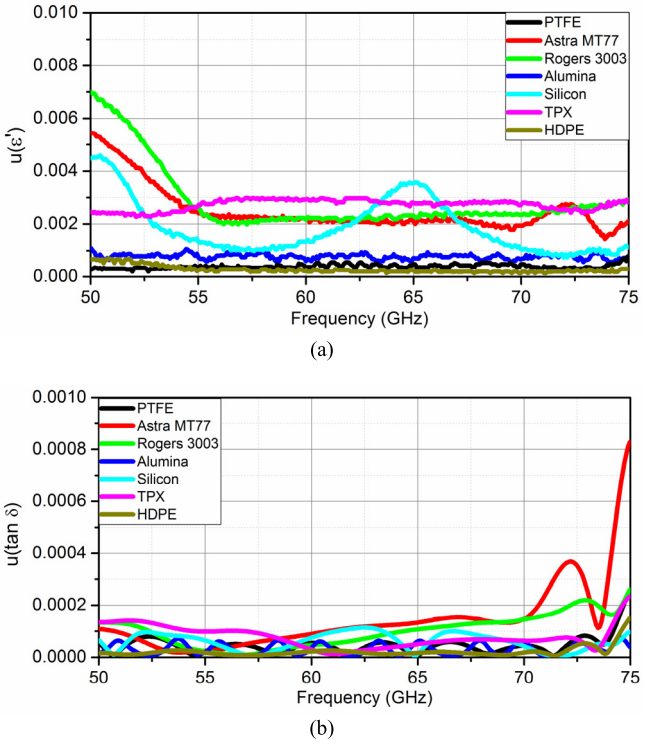

Fig. 8. Standard uncertainties based on the repeated measurements of the seven samples in Table I. (a) Dielectric constant ε'. (b) Loss tangent tanδ.

thickness, and the measured S-parameters of the sample. These estimates will be used to establish a preliminary assessment of the overall uncertainty of the MCK in the WR-15 waveguide band. This is not intended as a rigorous assessment of uncertainty, as this is beyond the scope of this article—rather, the intention is to provide an indication of the typical size of uncertainty that could be expected for these MCKs.

A. Insertion Repeatability

Random processes contribute to some errors in the extracted results. In this article, we consider two potential sources of such errors: 1) insertion repeatability of the sample, without changing the orientation of the sample in the MCK and 2) insertion repeatability that also includes changing the orientation of the sample with respect to its position in the sample holder. The former evaluation was performed on all samples; the latter evaluation was performed on just two of the PTFE samples of different thicknesses (i.e., 2.96 and 11.95 mm). Six repeated measurements were carried out on each individual sample, for both types of error evaluation (i.e., with and without changing the sample orientation between reinsertions). The two PTFE samples were marked so that their orientation could be changed in a systematic way (i.e., by introducing a rotation of 60° between each reinsertion).

Fig. 8 shows the calculated standard uncertainty in the extracted dielectric constant and loss tangent values, for the first investigation (i.e., for the random errors associated with the repeated measurements without changing the orientation of the sample). The standard uncertainty [34] for the extracted dielectric constant value $u(\varepsilon')$ was calculated using

$$u(\varepsilon') = \sqrt{\frac{1}{n(n-1)}\sum_{i=1}^{n}\left(\varepsilon_i' - \overline{\varepsilon'}\right)^2} \tag{8}$$

where n is the number of repeat measurements (in this case, $n = 6$), ε_i' is the extracted value for each repeated measurement, and $\overline{\varepsilon'}$ is the mean of the extracted values.

Similarly, the standard uncertainty for the loss tangent $u(\tan\delta)$ was calculated using

$$u(\tan\delta) = \sqrt{\frac{1}{n(n-1)}\sum_{i=1}^{n}(\tan\delta_i - \overline{\tan\delta})^2} \tag{9}$$

where $\tan\delta_i$ is the extracted value for each repeat measurement and $\overline{\tan\delta}$ is the mean of the extracted values.

The standard uncertainty values shown in Fig. 8 are less than 0.007 for the dielectric constant and less than 0.0008 for the loss tangent, at all frequencies and for all seven dielectric materials.

The investigation into changing the orientation of the two PTFE samples produced standard uncertainties of comparable size to those calculated for PTFE from the repeated measurements shown in Fig. 8. This indicates that the impact of changing the orientation of the PTFE sample in the MCK has negligible additional effect of the extracted values of dielectric constant and loss tangent for PTFE. This may not be the case for other materials (e.g., materials that exhibit some form of inhomogeneity) and so this type of assessment should be considered for all materials measured using the MCK.

B. Sample Thickness

In order to quantify the impact of sample thickness on the extracted dielectric constant and loss tangent values, measurements were made on four PTFE samples of different thicknesses: 2.96, 5.99, 8.99, and 11.95 mm. These samples were machined in the NPL workshops using a single PTFE rod and therefore were made from the same batch of material. The wavelength was calculated to be approximately 4.23 mm at 50 GHz, using a value of 2.008 for the dielectric constant of PTFE, as given in Table I. In general, characterization techniques based on free space or transmission line methods require that the samples under test should be thick enough to contain at least 20° of phase at the wavelength λ of interest. In our case, the thickness of the thinnest PTFE sample is 2.96 mm, which is significantly greater than the required minimum thickness of $20/360\cdot\lambda \approx 0.24$ mm.

Fig. 9 shows the extracted dielectric constant and loss tangent values for these four PTFE samples. Fig. 9 shows that there is no obvious correlation (i.e., systematic dependence) between the extracted dielectric constant and loss tangent values, and the thickness of the sample is measured. This suggests that this effect can be neglected for this material. This may not be the case for other materials (e.g., materials that exhibit either very high or very low loss) and so this type of assessment should be considered for all materials measured using the MCK.

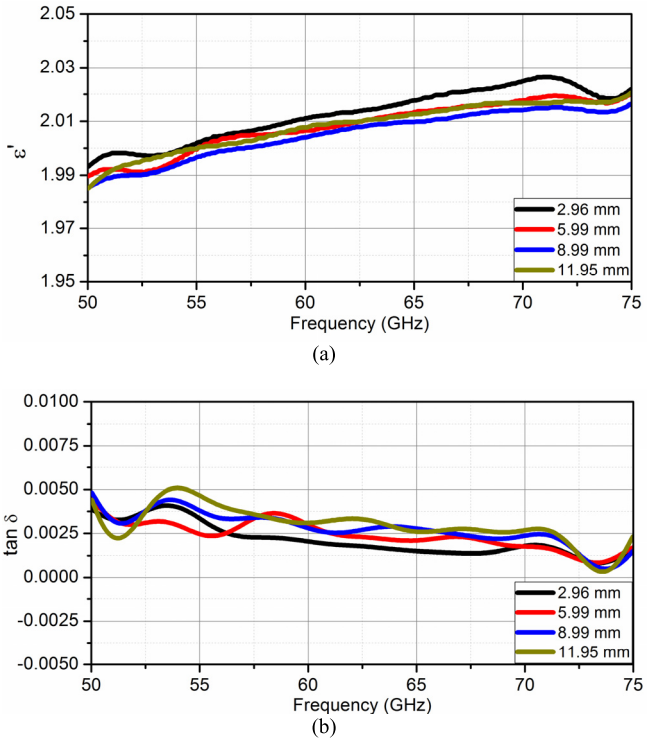

Fig. 9. Extracted (a) dielectric constant ε' and (b) loss tangent tanδ, for PTFE sample with the thicknesses of 2.96, 5.99, 8.99, and 11.95 mm using the NIST precision model (transmission only).

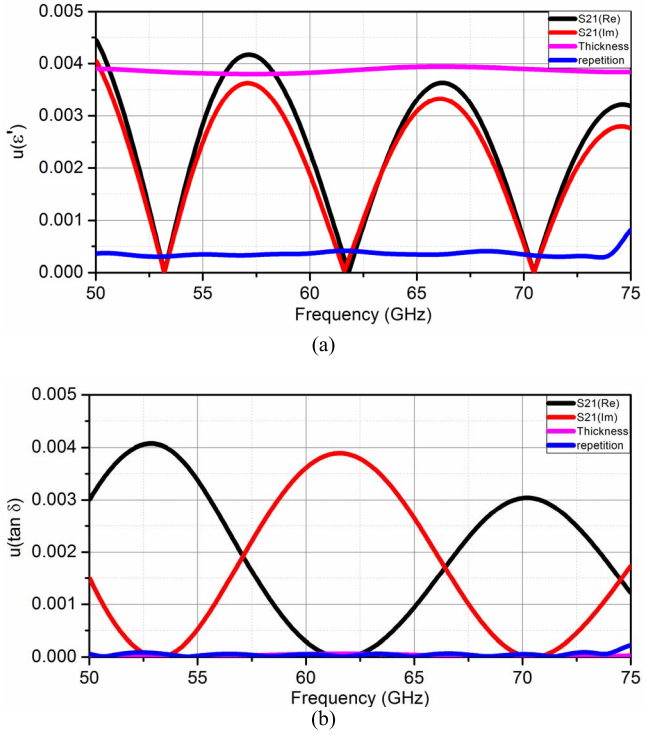

Fig. 10. Uncertainty components (expressed as standard uncertainties) for the PTFE sample of thickness 5.99 mm. (a) Dielectric constant ε'. (b) Loss tangent tanδ.

C. Sample Thickness Measurement

Part of the procedure for using the MCK requires a measurement of the thickness of the sample being measured. This is achieved using a digital micrometer that is included as part of the MCK. This thickness determination will be subject to error due to the accuracy of this digital micrometer. The digital readout on the micrometer introduces a digitizing error that is effectively half the resolution of the digital readout. For this MCK, the resolution of the micrometer is 0.01 mm and so the uncertainty due to this digitizing error is 0.01/2 mm $= 5\ \mu$m. It is further expected that any systematic errors in the digital micrometer will be less than 5 μm and so it is safe to assume that the total measurement error for the micrometer will not be greater than $(5 + 5)\ \mu\text{m} = 10\ \mu$m. This error can, therefore, be represented using a uniform (rectangular) distribution with a half-width of 10 μm. This is then converted to the equivalent standard uncertainty for a uniform distribution in the usual way [34] (i.e., by dividing the half-width by $\sqrt{3}$). The standard uncertainty in the thickness determination of each sample is therefore assumed to be $10/\sqrt{3}\ \mu\text{m} \approx 6\ \mu$m.

The impact due to the uncertainty in the measured sample thickness on the extracted dielectric constant and loss tangent is evaluated by perturbing the measured value for the thickness of the sample by the standard uncertainty and then reextracting the dielectric constant and loss tangent values. The difference between the two sets of extracted values (i.e., those obtained using the original value and the perturbed value for the sample thickness) is considered to represent the uncertainty due to the error in determining the sample thickness.

To illustrate this, the technique has been applied to the 5.99-mm-thick sample of PTFE. The impact of the standard uncertainty in the thickness determination on the extracted dielectric constant and loss tangent is shown in Fig. 10, where the associated standard uncertainty in the extracted dielectric constant and loss tangent is approximately 0.004 and 0.0001, respectively. Fig. 10 also shows the standard uncertainty due to the insertion repeatability (discussed previously) and the measured S-parameters (to be discussed next) for this sample.

D. S-Parameter Measurements

The MCK also makes use of measured values for S_{21} (or, equivalently, S_{12}) in order to extract the dielectric constant and loss tangent values for the sample. The NIST precision model (transmission only) was used to extract these values. In general, S-parameter measurements are affected by many different sources of uncertainty—e.g., the choice of calibration routine, the quality of the calibration standards, the type of transmission medium used for the measurements (i.e., free space or guided wave), the frequency range, the value of the device being measured, random effects, and so on. The overall uncertainty will depend on all these uncertainty contributions and so will usually have a different value at each measurement frequency. However, for the purposes of establishing a preliminary uncertainty budget for this MCK, it is considered adequate to use a single, typical, value of uncertainty for the measured S-parameter.

At WR-15 band, a single, typical, value of standard uncertainty for the measured S_{21} of a 20-dB attenuator ($|S_{21}| = 0.1$)

has been reported in [35] as 0.002 (in linear units). It is assumed that the uncertainty in S_{21} varies proportionally with $|S_{21}|$ (neglecting noise floor and dynamic range effects in the measurement system), and thus, for low-loss samples (where $|S_{21}| \approx 1$), the uncertainty will be of the order of 0.02. It is further assumed that this uncertainty applies equally to both the real and imaginary components of S_{21}—i.e., the uncertainty can be represented by a circular region of uncertainty in the complex S_{21} plane. This method is often used for dealing with uncertainties in complex-valued measurements and is explained in more detail in [36]. A more detailed treatment of the uncertainty in the S-parameters can be obtained by applying the techniques given in [37] and [38].

The impact of the uncertainty in S_{21} on the extracted dielectric constant and loss tangent is evaluated in a similar way to the uncertainty in the sample thickness determination, as described earlier (i.e., by perturbing each value by its standard uncertainty). The process is applied, in turn, to both the real and imaginary components of the measured S_{21}—i.e., the real component is perturbed by the standard uncertainty, and then, the imaginary component is perturbed by the same standard uncertainty. In each case, the change in the extracted dielectric constant and loss tangent is considered to represent the uncertainty due to the errors in both the real and imaginary components of S_{21}.

As mentioned earlier, this technique has been applied to the 5.99-mm-thick sample of PTFE. The impact of the standard uncertainty in the real and imaginary components of S_{21} (using a value for the uncertainty of 0.02 for both components) on the extracted dielectric constant and loss tangent is shown in Fig. 10.

E. Combined Uncertainty

Having evaluated the standard uncertainty due to each of the main sources of error, these uncertainty contributions can be combined to provide an overall uncertainty in the extracted dielectric constant and loss tangent values.

For m uncertainty contributions, u_i ($i = 1$ to m), the combined standard uncertainty u_c can be established using [34]

$$u_c = \sqrt{\sum_{i=1}^{m} u_i^2}. \tag{10}$$

The use of this equation assumes that u_i are independent of each other (i.e., there is no correlation between the sources of uncertainty). For the preliminary assessment of uncertainty reported here, $m = 4$, since we are considering only four sources of uncertainty; u_1 is the uncertainty associated with the insertion repeatability of the sample, u_2 is the uncertainty associated with the measurement of the thickness of the sample, u_3 is the uncertainty associated with the real component of S_{21}, and u_4 is the uncertainty associated with the imaginary component of S_{21}.

Having established a value of u_c for the extracted dielectric constant and a value of u_c for the loss tangent, it is usual to use these combined standard uncertainties to derive the expanded uncertainties for both extracted quantities at a specified coverage probability. The expanded uncertainty provides an interval that is expected to include a large proportion of the values that can be attributed to the true value of the extracted quantity.

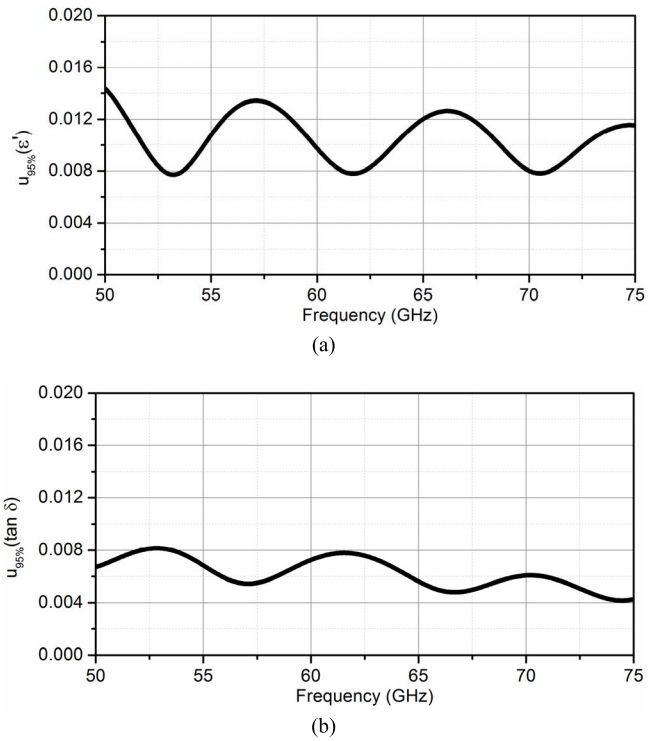

Fig. 11. Expanded uncertainty (at a 95% coverage probability) for the PTFE sample of thickness 5.99 mm. (a) Dielectric constant ε'. (b) Loss tangent tanδ.

For a given combined standard uncertainty u_c, the expanded uncertainty U is established using

$$U = ku_c \tag{11}$$

where k is a coverage factor chosen so that the expanded uncertainty interval contains the true value at a specified coverage probability. In many measurement situations, it is often reasonable to assume that when $k = 2$, the coverage probability for the expanded uncertainty is of the order of 95%.

Fig. 11 shows the expanded uncertainty with a 95% coverage probability $U_{95\%}$ as a function of frequency for the extracted values of both the dielectric constant and loss tangent for the 5.99-mm-thick sample of PTFE. This is based on the combined effects due to the four uncertainty components considered in this article.

F. Discussion

The abovementioned uncertainty investigation shows that the impact of systematic errors (due to the measurement of the thickness of the sample and the measured S-parameters of the sample) on the extracted material properties is greater than the impact of the random errors. Similar observations, concerning experimentally determined values for materials parameters, have been reported elsewhere [3]. Since systematic errors dominate the overall uncertainty in the extracted materials parameters, it is important to acquire both accurate S-parameter measurements and accurate length determinations for the sample of material being measured.

The values of uncertainty established using the abovementioned uncertainty analysis apply only to the sample of PTFE considered in this article. The values do not apply to other materials, including the other materials in this article. Such uncertainty estimates need to be established on a case-by-case basis since each uncertainty contribution is likely to change for each given material.

It must also be emphasized that the uncertainty estimates established in this article are only preliminary estimates intended to give an indication of the likely uncertainty achievable using these MCKs. In practice, the uncertainty will depend on many factors, including the value of the sample being measured. Also, MCKs operating in different waveguide bands (i.e., at different frequencies) will have very different values of uncertainty.

V. Conclusion

This article has presented an in-depth study on the simple VNA-based material characterization technique using MCKs. Seven different types of low-loss dielectric materials were measured using such an MCK operating at 50–75 GHz, and the extracted dielectric constant and loss tangent values show good agreement with values published in the open literature. Uncertainties in the measurement results were also investigated and discussed. This article demonstrates that the new method based on MCK is an attractive alternative approach to the conventional free-space technique, for material characterization at millimeter-wave and terahertz frequencies.

Acknowledgment

Y. Wang would like to thank the studentship provided by the Nanjing University of Science and Technology, Nanjing, China.

References

[1] S. Kim, D. Novotny, J. Gordon, and J. Guerrieri, "A free-space measurement method for the low-loss dielectric characterization without prior need for sample thickness data," *IEEE Trans. Antennas Propag.*, vol. 64, no. 9, pp. 3869–3879, Sep. 2016.

[2] A. Kazemipour *et al.*, "Design and calibration of a compact quasi-optical system for material characterization in millimeter/submillimeter wave domain," *IEEE Trans. Instrum. Meas.*, vol. 64, no. 6, pp. 1438–1445, Jun. 2015.

[3] R. N. Clarke *et al.*, "A guide to the characterisation of dielectric materials at RF and microwave frequencies," Published Inst. Meas. Control (UK)/Nat. Phys. Lab., New Delhi, India, Tech. Rep., 2003.

[4] A. N. Al-Omari and K. L. Lear, "Dielectric characteristics of spin-coated dielectric films using on-wafer parallel-plate capacitors at microwave frequencies," *IEEE Trans. Dielectr. Electr. Insul.*, vol. 12, no. 6, pp. 1151–1161, Dec. 2005.

[5] A. Mirbeik-Sabzevari and N. Tavassolian, "Characterization and validation of the slim-form open-ended coaxial probe for the dielectric characterization of biological tissues at millimeter-wave frequencies," *IEEE Microw. Wireless Compon. Lett.*, vol. 28, no. 1, pp. 85–87, Jan. 2018.

[6] P. M. Meaney, A. P. Gregory, J. Seppälä, and T. Lahtinen, "Open-ended coaxial dielectric probe effective penetration depth determination," *IEEE Trans. Microw. Theory Techn.*, vol. 64, no. 3, pp. 915–923, Mar. 2016.

[7] S. Zinal and G. Boeck, "Complex permittivity measurements using TE_{11p} modes in circular cylindrical cavities," *IEEE Trans. Microw. Theory Techn.*, vol. 53, no. 6, pp. 1870–1874, Jun. 2005.

[8] E. Massoni, G. Siciliano, M. Bozzi, and L. Perregrini, "Enhanced cavity sensor in SIW technology for material characterization," *IEEE Microw. Wireless Compon. Lett.*, vol. 28, no. 10, pp. 948–950, Oct. 2018.

[9] M. Naftaly, N. Shoaib, D. Stokes, and N. M. Ridler, "Intercomparison of terahertz dielectric measurements using vector network analyzer and time-domain spectrometer," *J. Infr. Milli. THz Waves*, vol. 37, no. 7, pp. 691–702, Jul. 2016.

[10] A. P. Toda and F. D. Flaviis, "60-GHz substrate materials characterization using the covered transmission-line method," *IEEE Trans. Microw. Theory Techn.*, vol. 63, no. 3, pp. 1063–1075, Mar. 2015.

[11] E. Hajisaeid, A. F. Dericioglu, and A. Akyurtlu, "All 3-D printed free-space setup for microwave dielectric characterization of materials," *IEEE Trans. Instrum. Meas.*, vol. 67, no. 8, pp. 1877–1886, Aug. 2018.

[12] X. Zhang *et al.*, "A free-space measurement technique of terahertz dielectric properties," *J. Infr., Millim., THz. Waves*, vol. 38, no. 3, pp. 356–365, Mar. 2017.

[13] A. La Gioia *et al.*, "Open-ended coaxial probe technique for dielectric measurement of biological tissues: Challenges and common practices," *Diagnostics*, vol. 8, no. 2, p. 40, Jun. 2018.

[14] T. Tosaka, K. Fujii, K. Fukunaga, and A. Kasamatsu, "Development of complex relative permittivity measurement system based on free-space in 220–330-GHz range," *IEEE Trans. Terahertz Sci. Technol.*, vol. 5, no. 1, pp. 102–109, Jan. 2015.

[15] M. Naftaly and R. E. Miles, "Terahertz Time-domain spectroscopy for material characterization," *Proc. IEEE*, vol. 95, no. 8, pp. 1658–1665, Aug. 2007.

[16] M. Naftaly, R. G. Clarke, D. A. Humphreys, and N. M. Ridler, "Metrology state-of-the-art and challenges in broadband phase-sensitive terahertz measurements," *Proc. IEEE*, vol. 105, no. 6, pp. 1151–1165, Jun. 2017.

[17] T. Ozturk, O. Morikawa, I. Ünal, and İ. Uluer, "Comparison of free space measurement using a vector network analyzer and low-cost-type THz-TDS measurement methods between 75 and 325 GHz," *J. Infr. Millim. THz Waves*, vol. 38, no. 10, pp. 1241–1251, Oct. 2017.

[18] A. Khalid, D. Cumming, R. Clarke, C. Li, and N. Ridler, "Evaluation of a VNA-based material characterization kit at frequencies from 0.75 THz to 1.1 THz," in *Proc. IEEE 9th UK-Eur.-China Workshop Millimetre Waves THz. Technol. (UCMMT)*, Qingdao, China, Sep. 2016, pp. 31–34.

[19] J.-H. Lee, J. M. Lee, and K. C. Hwang, "Sector-beam antennas for wide detection area in 79 GHz automotive short range radar(SRR) sensor," in *Proc. IEEE Asia–Pacific Microw. Conf. (APMC)*, Nov. 2018, pp. 399–401.

[20] G. I. Kiani, T. S. Bird, and K. Lee Ford, "60 GHz ASK modulator using switchable FSS," in *Proc. IEEE Antennas Propag. Soc. Int. Symp. (APSURSI)*, Jul. 2010, pp. 1–4.

[21] A. Dimitriades and R. Divorne, "MCK User Guide—Version 1.1," Swissto12 SA, Renens, Switzerland, Tech. Rep. Swissto12, 2018.

[22] R. J. Wylde, "Millimetre-wave Gaussian beam-mode optics and corrugated feed horns," *IEE Proc. H Microw., Opt. Antennas*, vol. 131, no. 4, pp. 258–262, Aug. 1984.

[23] P. G. Bartley and S. B. Begley, "Improved free-space S-parameter calibration," in *Proc. IEEE Instrum. Meas. Technol. Conf.*, Ottawa, ON, Canada, May 2005, pp. 372–375.

[24] J. Baker-Jarvis, E. J. Vanzura, and W. A. Kissick, "Improved technique for determining complex permittivity with the transmission/reflection method," *IEEE Trans. Microw. Theory Techn.*, vol. 38, no. 8, pp. 1096–1103, Aug. 1990.

[25] S. Rajesh, V. S. Nisa, K. P. Murali, and R. Ratheesh, "Microwave dielectric properties of PTFE/rutile nanocomposites," *J. Alloys Compounds*, vol. 477, nos. 1–2, pp. 677–682, May 2009.

[26] Y. Yamaguchi and Y. Sato, "Measuring method of complex dielectric constant with monostatic horn antenna in W-band using multiple distance measurements and analysis," in *Proc. IEEE Asia–Pacific Microw. Conf. (APMC)*, Kuala Lumpar, Malaysia, Nov. 2017, pp. 666–669.

[27] L. Martin *et al.*, "Attenuation of high frequency signals in structured metallization on glass: Comparing different metallization techniques with 24 GHz, 77 GHz and 100 GHz structures," in *Proc. IEEE 69th Electron. Compon. Technol. Conf. (ECTC)*, May 2019, pp. 726–732.

[28] P. I. Dankov, "Dielectric anisotropy of modern microwave substrates," in *Microwave and Millimeter Wave Technologies from Photonic Bandgap Devices to Antenna and Applications*, Igor Minin Ed. Rijeka, Croatia: InTech, 2010.

[29] H. D. Hristov, J. M. Rodriguez, and W. Grote, "The grooved-dielectric Fresnel zone plate: An effective terahertz lens and antenna," *Microw. Opt. Technol. Lett.*, vol. 54, no. 6, pp. 1343–1348, Jun. 2012.

[30] K. Zhou, S. Caroopen, Y. Delorme, M. Batrung, M. Gheudin, and S. Shi, "Dielectric constant and loss tangent of silicon at 700–900 GHz at cryogenic temperatures," *IEEE Microw. Wireless Compon. Lett.*, vol. 29, no. 7, pp. 501–503, Jul. 2019.

[31] Elhawil, L. Zhang, and J. Stiens, "A quasi-optical free-space method for dielectric constant characterization of polymer materials in mm-wave band," in *Proc. Symp. IEEE/LEOS Benelux Chapter*, Brussels, Belgium, Dec. 2007, pp. 187–190.
[32] K. Z. Rajab *et al.*, "Broadband dielectric characterization of aluminum oxide (AI203)," *J. Microelectron. Electron. Packag.*, vol. 5, no. 1, pp. 101–106, 2008.
[33] P. H. Bolivar *et al.*, "Measurement of the dielectric constant and loss tangent of high dielectric-constant materials at terahertz frequencies," *IEEE Trans. Microw. Theory Techn.*, vol. 51, no. 4, pp. 1062–1066, Apr. 2003.
[34] Joint Committee for Guides in Metrology (JCGM/WG 1), *Evaluation of Measurement Data—Guide to the Expression of Uncertainty in Measurement*, 1st ed., document JCGM 100:2008, Bureau International des Poids et Measures (BIPM), Sep. 2008.
[35] N. M. Ridler, "News in RF impedance measurements," in *Proc. 27th Gen. Assem. Int. Union Radio Sci. (URSI)*, Aug. 2002, pp. 1–4.
[36] N. M. Ridler and J. C. Medley, *An Uncertainty Budget for VHF and UHF Reflectometers*, vol. 120. National Physical Laboratory, London, U.K., May 1992.
[37] N. M. Ridler and M. J. Salter, "An approach to the treatment of uncertainty in complex S-parameter measurements," *Metrologia*, vol. 39, no. 3, pp. 295–302, 2002.
[38] N. M. Ridler and M. J. Salter, "Evaluating and expressing uncertainty in high-frequency electromagnetic measurements: A selective review," *Metrologia*, vol. 51, no. 4, p. S191, Jul. 2014.

Yi Wang (S'19) received the B.Eng. degree from Anqing Normal University, Anqing, China, in 2016. She is currently pursuing the Ph.D. degree with the Nanjing University of Science and Technology (NUST), Nanjing, China.

From January 2019 to July 2019, she was a Visiting Researcher with the Department of Electromagnetic and Electrochemical Technologies, National Physical Laboratory, Teddington, U.K., where she was involved in high-frequency electromagnetic measurement. Her current research interests include radio-frequency integrated circuits, microwave passive devices, and microwave measurements.

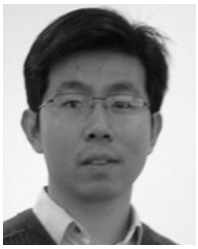

Xiaobang Shang (M'13–SM'19) received the B.Eng. degree (Hons.) in electronics and communication engineering from the University of Birmingham, Birmingham, U.K., in 2008, the B.Eng. degree in electronics and information engineering from the Huazhong University of Science and Technology (HUST), Wuhan, China, in 2008, and the Ph.D. degree in microwave engineering from the University of Birmingham in 2011.

He is currently a Senior Research Scientist with the National Physical Laboratory (NPL), Teddington, U.K. He has authored or coauthored over 70 scientific articles on microwave measurements and microwave circuits.

Dr. Shang was a recipient of several prestigious awards, including the ARFTG Microwave Measurement Student Fellowship Award in 2009, the IEEE Tatsuo Itoh Award in 2017, and the ARMMS Steve Evans-Pughe Prize in 2017.

Nick M. Ridler (M'03–SM'06–F'14) received the B.Sc. degree from King's College London, University of London, London, U.K., in 1981.

He is currently the Head of Science at the Department of Electromagnetic and Electrochemical Technologies, National Physical Laboratory, Teddington, U.K. He is also a Visiting Professor with the University of Leeds, Leeds, U.K., the University of Liverpool, Liverpool, U.K., and the University of Surrey, Guildford, U.K., and the Non-Executive Director of LA Techniques Ltd., Surbiton, U.K. He has more than 35 years' experience working in industrial, government, and academic research establishments. His main area of interest is precision high-frequency electromagnetic measurement (from 1 kHz to 1 THz).

Prof. Ridler is a fellow of the Institution of Engineering and Technology (IET) and the Institute of Physics (IOP).

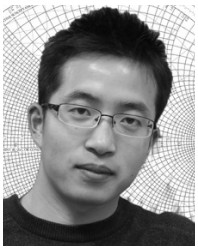

Tongde Huang received the Ph.D. degree from the Department of Electronics and Computer Engineering, The Hong Kong University of Science and Technology, Hong Kong, in 2013.

From 2014 to 2017, he was with the Microwave Electronics Laboratory Group, Chalmers University of Technology, Gothenburg, Sweden. He is currently with the Nanjing University of Science and Technology, Nanjing, China.

Wen Wu (SM'10) received the Ph.D. degree in electromagnetic field and microwave technology from Southeast University, Nanjing, China, in 1997.

He is currently a Professor with the School of Electronic and Optical Engineering, Nanjing University of Science and Technology, Nanjing. His current research interests include microwave and millimeter-wave theories and technologies, microwave and millimeter-wave detection, and multimode compound detection. He holds 14 patents. He has authored or coauthored over 240 journal articles and conference papers.

Prof. Wu has received six times of Ministerial- and Provincial-Level Science and Technology Awards.